doi: 10.82124/CEAS-GNC-2026-001 CEAS-GNC-2026-001

EuroGNC Navigation Guidance Control CEAS Madrid, Spain May 5th-7th uc3m Universidad Carlos III de Madrid AIAA 2026

Parallel Transport of a Velocity Frame for Point Mass 3-DOF Lifting Vehicle Modeling

Florian Dietrich Research Engineer, Université Paris Saclay, ONERA, DTIS, 91123, Palaiseau, France. florian.dietrich@onera.fr

Ioannis Sarras Research Engineer, Université Paris Saclay, ONERA, DTIS, 91123, Palaiseau, France. ioannis.sarras@onera.fr

ABSTRACT

This paper proposes a new formulation for modeling 3-DOF lifting vehicles in Cartesian coordinates. We address the problem of describing the lift force as orthogonal to velocity vector of the vehicle, which is not well-defined in traditional models. In spherical coordinates there is a singularity in vertical flight whereas in Cartesian coordinates, using a reference direction to define the lift vector also introduces a singularity. The proposed approach consists of a moving frame carried along the trajectory by parallel transport, with its first axis remaining co-linear to the velocity vector. The other two vectors are orthogonal to the velocity vector at all time and are used to express the lift force in a well-defined manner. The advantages of this approach are illustrated in the simulation of a simplified vehicle performing a looping.

Keywords: Parallel Transport Frame, Singularities, 3-DOF Models

Nomenclature

Ω	=	rotation vector of the parallel transport frame
$\Omega_\times$	=	skew symmetric matrix of the cross product by rotation vector Ω
λ, δ, R	=	geographic coordinates (latitude, longitude, distance to the center of the Earth)
γ, χ, V	=	velocity vector in spherical coordinates (flight path angle, heading, norm)
σ	=	bank angle
ρ	=	air density
C_D, C_L	=	drag and lift coefficient
D, L	=	magnitude of the drag and lift acceleration
$R_v(\alpha)$	=	axis-angle rotation matrix of angle α around vector v
A_{ref}	=	aerodynamic reference area
e_1, e_2, e_3	=	vectors of the velocity parallel transport frame
l_2, l_3	=	components of the lift vector in the velocity parallel transport frame
m	=	vehicle's mass
r, v	=	Cartesian coordinates (position vector relative to the center of the Earth, velocity vector)
$\dot{}$	=	time derivative
$'$, $''$	=	first and second derivative
$\times, \cdot$	=	vector cross and dot product

1 Introduction

This article is about modeling a 3-DOF aerospace vehicle as a point-mass object subject to aerodynamic forces, lift in particular. Theses models are typically used for simulation and trajectory generation, trajectory optimization, guidance law design and performance assessment. However, the lift force is not-well defined everywhere on the state-space of this models due to singularities. To address this issue, we propose an approach using Cartesian coordinates and parallel transport frames to properly define the lift force along all trajectories.

This paper is organized in the following way. A brief review of existing 3-DOF models for lifting vehicles is given Section 2, mainly the spherical and Cartesian coordinates models and their respective singularities. In Section 3, the classical Frenet-Serret frame is recalled along with the parallel transport frame. A comparison of both frames is presented to exhibit the advantages of the parallel transport frame. The main contribution of this paper is stated in Section 4. It consists in adding a parallel transport frame to the Cartesian dynamics of a lifting vehicle. This allows a well-defined expression of the lift force in this frame, without the singularities of the previously presented models. Section 5 consists of an illustrative example of a vehicle performing a looping. Finally, Section 6 concludes this paper and gives some ideas for future works.

2 Review of 3-DOF models for lifting vehicles

This section presents existing 3-DOF of aerospace vehicle models [1], with a focus on singularities and the modelling of the lift. For simplicity, and without loss of generality, the Earth is considered non-rotating, the gravity Newtonian and the vehicle is not propelled.

One of the most common model used in the literature to describe a lifting vehicle is the geographic coordinates model, which uses spherical coordinates to describe the position and velocity of the vehicle. It is recalled below.

Definition 1 (Dynamics in spherical coordinates)**.** *For a non-rotating Earth with Newtonian gravity, the 3-DOF equations of motion of a lifting vehicle in spherical coordinates are given by :*

$$\begin{aligned}
\dot{R} &= V \sin\gamma, \\
R\cos\delta\,\dot{\lambda} &= V \sin\chi\,\cos\gamma, \\
R\,\dot{\delta} &= V\cos\chi\cos\gamma, \\
\dot{V} &= -D - \sin\gamma\,\frac{\mu}{R^2}, \\
V\,\dot{\gamma} &= L\cos\sigma + \left(\frac{V^2}{R} - \frac{\mu}{R^2}\right)\cos\gamma, \\
V\cos\gamma\,\dot{\chi} &= L\sin\sigma + \frac{V^2}{R}\cos^2\gamma\tan\delta\sin\chi,
\end{aligned} \tag{1}$$

with the lift and drag accelerations

$$L = \frac{1}{2}\,\rho\,V^2\,\frac{A_{ref}\,C_L}{m}, \tag{2}$$

$$D = \frac{1}{2}\,\rho\,V^2\,\frac{A_{ref}\,C_D}{m}. \tag{3}$$

In spherical coordinates the lift force is always normal to the velocity vector by construction. However this model suffers from singularities in position at the poles ($\delta = \pm\pi/2$) as well as for a purely vertical velocity vector ($\gamma = \pm\pi/2$). They can be tackled by a new coordinate chart that shifts away the singularities [2] (e.g. from vertical to horizontal velocity) but this does not remove the singularities. A

mechanism to switch charts near a singularity is then required so that a valid map is always used for each part the trajectory. In addition, there is also a singularity at zero velocity that has to be taken into account, but this is outside of the scope of this paper.

An alternative is to use Cartesian coordinates to represent the position and velocity of the vehicle, as presented below.

Definition 2 (Dynamics in Cartesian coordinates)**.** *For a non-rotating Earth, the 3-DOF equations of motion of a lifting vehicle in cartesian coordinates are given by :*

$$\begin{aligned} \dot{r} &= v, \\ \dot{v} &= a_G + a_L + a_D, \end{aligned} \tag{4}$$

where $r \in \mathbb{R}^3$ is the position vector relative to the center of the Earth, $v \in \mathbb{R}^3$ the velocity vector, and a_G, a_L, a_D are respectively the gravity, lift and drag acceleration vectors.

The Cartesian coordinates model in itself has no singularity, but defining the lift in these coordinates is not intuitive. A more practical lift vector can be constructed using a reference direction e_{ref} [2–5] and the normalized velocity vector $\bar{v}$ such that

$$a_L = L\, R_{\bar{v}}(\sigma)\, \bar{v} \times (e_{ref} \times \bar{v}), \tag{5}$$

where σ is the same bank angle as in the spherical coordinates model (1) when the reference direction is the local upward vertical, and where $R_{\bar{v}}(\sigma)$ is the axis-angle rotation matrix of angle σ around vector $\bar{v}$. However, the lift vector is null when e_{ref} and $\bar{v}$ are colinear, which restricts its use. This issue can be alleviated by choosing another reference direction. This in turn requires a mechanism to switch reference direction whenever necessary, which is not well-suited for all applications.

When possible, the orthogonality property of the lift and velocity can also be introduced as a constraint

$$a_L{}^{\top}\, v = 0. \tag{6}$$

However, this is not a viable choice for trajectory optimization with direct methods since the constraints are only enforced at the sample times and not in between, resulting in discrepancies between the continuous time dynamics and the sampled trajectory solution of the direct optimization [6].

In Cartesian 6-DOF models, the lift vector is expressed without singularities using the body frame of the vehicle [1]. However, this requires computing the moments of all the forces with respect to the center of gravity of the vehicle, which adds an unwanted layer of complexity.

The modeling contribution of this paper is inspired by the 6-DOF case but without the complexity of the moment equation. It is based on parallel transport frames, which are a way of framing a curve and are presented next.

3 Curve framing and parallel transport frames

The Frenet-Serret frame [7, 8] is a classical way of framing a curve, see [9] for a modern presentation, from which the following definition is derived.

Definition 3 (Frenet-Serret frame)**.** *Let $r(s)$ be a twice differentiable arc-length parametrized curve in $\mathbb{R}^3$, meaning the velocity $\|r'(s)\| = 1$ at all times $s \in [0, 1]$. The three vectors forming the frame are the tangent vector T, normal vector N and binormal vector B, and are defined as*

$$T = r', \qquad N = \frac{r''}{\|r''\|}, \qquad B = T \times N, \tag{7}$$

where $\|r''\|$ is called the curvature and denoted κ. Along the curve, the three vectors of the Frenet-Serret frame also satisfy the differential equations

$$\begin{pmatrix} T' \\ N' \\ B' \end{pmatrix} = \begin{pmatrix} 0 & \kappa & 0 \\ -\kappa & 0 & \tau \\ 0 & -\tau & 0 \end{pmatrix} \begin{pmatrix} T \\ N \\ B \end{pmatrix}, \tag{8}$$

where τ is the torsion.

However, the Frenet-Serret frame is not defined on zero curvature points and segments (inflexion points and straight lines). This also yields discontinuities of the frame vectors along a curve and restricts its application to general curves. Figure 1a shows the N and B vectors of the Frenet-Serret frames along three joined cubic Bézier curves containing an inflexion point and a straight segment. The frames are discontinuous around the inflexion point and not defined on the straight segment.

Parallel transport frames were then proposed by Bishop in [10] to remove these singularities. Klok later described the frame's evolution along a curve with a differential equation in [11], from which the following definition is inspired.

Definition 4 (Parallel transport frame)**.** *The parallel transport frame of a twice differentiable arc-length parametrized curve $r(s)$ in $\mathbb{R}^3$ satisfies the differential equation*

$$R' = \Omega_\times R, \tag{9}$$

where the columns of the rotation matrix $R \in \mathrm{SO}(3)$ are the unit vectors (e_1, e_2, e_3) of the frame, and $\Omega_\times$ is the skew symmetric matrix of the rotation vector Ω defined as

$$\Omega = r' \times r''. \tag{10}$$

The first vector of the parallel transport frame e_1 is initialized with the initial velocity vector $r'(0)$ and the other remaining initial conditions of vectors e_2 and e_3 are chosen freely to form an orthonormal basis.

The parallel transport frame is well-defined on arc-length parametrized curves, even on straight segments and inflexion points. The first vector e_1 always stays colinear to the velocity vector r' and the orthonormal property of matrix R is preserved along the trajectory, see [11] for the proofs.

Figure 1b shows the e_2 and e_3 vectors of a parallel transport frame along three joined cubic Bézier curves containing an inflexion point and a straight segment. The frame was initialized as a Frenet-Serret frame because it is well-defined initially. The parallel transport frames does not exhibit any of the discontinuities of the Serret-Frenet frames of Figure 1a.

In [12], the authors gave a simple and fast numerical scheme based on a double reflection for computing the parallel transport frame along a known curve, with the same accuracy as a 4th order Runge-Kutta method.

Guggenheimer showed in [13] that the difference (in rotation) between parallel transport and Frenet-Serret frames can be computed using the torsion τ. However, this reintroduces the singularity of the Frenet-Serret frame and the associated discontinuities.

Parallel transport frames are also rotation minimizing frames [14], along with Frenet-Serret frames and osculating frames [15].

In general, parallel transport frames are not periodic along a closed curve, but they can be made periodic by adding an additional rotation [16]. However this approach is also based on the Frenet-Serret frame and re-introduces its singularities.

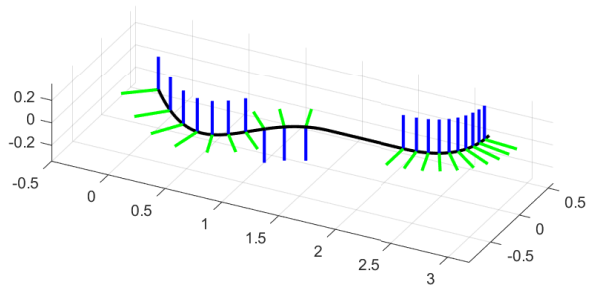

(a) The Frenet-Serret frames are discontinuous around inflexion points and undefined on straight segments.

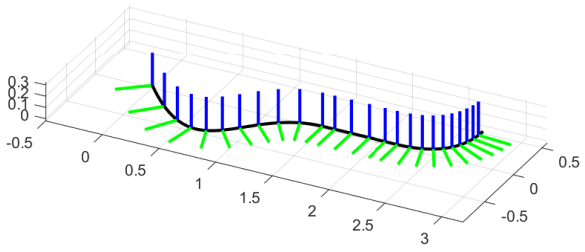

(b) The parallel transport frames are continuous and well-defined on inflexion points and straight segments.

Fig. 1 Comparison of Frenet-Serret (a) and parallel transport frames (b) along three joined cubic Bézier curves. The tangent vectors are omitted for clarity.

Parallel transport frames are, for example, used in computer graphics for surface sweeping [17], and in path-generation and path-following algorithms in robotics and for UAVs [18–20].

The contribution of this paper is then stated in the following section.

4 Parallel transport frame for lift modeling

The main idea of the paper is to use a parallel transported frame along the trajectory of the vehicle to express the lift vector properly. The parallel transport frame was previously defined for arc-length parametrized curves for which $||v|| = 1$ at all times. This assumption can be relaxed to non-zero velocity trajectories, stated as follows, and assumed to hold for the remaining of the paper.

Assumption 1. *The vehicle follows a trajectory where its velocity never cancels, ie*

$$\forall\, t \in [t_0, t_f],\ V(t) = \|v(t)\| > 0. \tag{11}$$

The proposed model then consists in adding the dynamics of three orthonormal vectors e_1, e_2 and e_3 to the Cartesian dynamics (4). These vectors are defined as the columns of a rotation matrix

$$R = [e_1\ e_2\ e_3], \tag{12}$$

with an initial condition denoted

$$R(t_0) = R_0 \in \mathrm{SO}(3), \tag{13}$$

such that, in particular

$$e_1(t_0) = \frac{v(t_0)}{\|v(t_0)\|}. \tag{14}$$

This means that the first vector is initially colinear with the velocity vector of the vehicle. The other two vectors can be chosen freely to form an orthonormal basis and are used to express the lift vector.

The following proposition details the dynamics of the parallel transport frame and its use for defining the lift.

Proposition 1. *Let the system with Cartesian dynamics* (4) *be augmented with*

$$\dot{R} = \Omega_{\times} R, \tag{15}$$

where

$$\Omega = \frac{v}{\|v\|} \times \frac{\dot{v}}{\|v\|}, \tag{16}$$

and with initial conditions (13) *and* (14)*, then the lift acceleration vector defined as*

$$a_L = l_2\, e_2 + l_3\, e_3, \tag{17}$$

is well-defined along any trajectory satisfying Assumption 1.

Proof. We first rewrite the elements of the proof from [11] with the notation of this paper to show that the parallel transport frame obeying (15) with initial condition (13) and (14) is an orthonormal frame, with the first vector being colinear to the velocity vector.

From (15), the dynamics of the vectors of the parallel transport frame writes

$$\dot{e}_i = \Omega \times e_i, \quad i \in \{1, 2, 3\}. \tag{18}$$

Then, let us show that the normalized velocity vector follows the same dynamics as the vectors of the parallel transport frame, namely

$$\frac{\mathrm{d}}{\mathrm{d}t}\left(\frac{v}{\|v\|}\right) = \Omega \times \frac{v}{\|v\|} \tag{19}$$

On the one hand, by differentiation of the normalized velocity vector with respect to time we get

$$\frac{\mathrm{d}}{\mathrm{d}t}\left(\frac{v}{\|v\|}\right) = \frac{1}{\|v\|^2}\left(\dot{v}\,\|v\| - v\,\frac{v^{\top}\dot{v}}{\|v\|}\right) = \left(I - \frac{v\,v^{\top}}{\|v\|^2}\right)\frac{\dot{v}}{\|v\|}. \tag{20}$$

On the other hand, replacing Ω by its definition (16) in the left hand side of (19) yields

$$\Omega \times \frac{v}{\|v\|} = \left(\frac{v}{\|v\|} \times \frac{\dot{v}}{\|v\|}\right) \times \frac{v}{\|v\|} = \left(\frac{v}{\|v\|} \cdot \frac{v}{\|v\|}\right)\frac{\dot{v}}{\|v\|} - \left(\frac{v}{\|v\|} \cdot \frac{\dot{v}}{\|v\|}\right)\frac{v}{\|v\|}, \tag{21}$$

which is a vector triple product that has been rewritten in terms of dot products. By seeing that $v \cdot v = \|v^2\|$ and by rearranging the terms, one obtains (20).

Since in (14) the first vector of the frame e_1 is initialized as the initial normalized velocity vector and since it follows the same differential equation, they are equal at all times.

The same argument is made about the remaining vectors e_2 and e_3 which are initially orthogonal to the initial velocity vector, hence are orthogonal to the velocity vector for all time.

As in [11], the e_i vectors are proved to be unit vectors by showing that

$$\frac{\mathrm{d}}{\mathrm{d}t}\left(\|e_i\|^2\right) = \frac{\mathrm{d}}{\mathrm{d}t}\left(e_i \cdot e_i\right) = 2\, e_i \cdot \dot{e}_i = 0, \quad i \in \{1, 2, 3\}. \tag{22}$$

This ensures that by defining the lift vector in the (e_2, e_3) plane as in (17), then it remains normal to the velocity vector at all times and is thus well-defined. ■

We then make several remarks about the proposed model. First, we see that when the total acceleration of the vehicle $\dot{v}$ is null or colinear with the velocity v, the rotation vector Ω defined in (16) is null and thus from (15) the frame R stays constant.

For computational efficiency, only the two velocity-normal vectors e_2 and e_3 can be considered because e_1 can be recovered from the normalized velocity vector. Their separate dynamics, as given in [11], can also be written

$$\dot{e}_2 = -\, {e_2}^\top \frac{\dot{v}}{\|v\|} \frac{v}{\|v\|}, \qquad \dot{e}_3 = -\, {e_3}^\top \frac{\dot{v}}{\|v\|} \frac{v}{\|v\|} \tag{23}$$

A further reduction of the number of variables can be achieved by considering only one of the velocity-normal vectors plus an angle μ. This angle is similar to the bank angle σ in (5) except it is not periodic [16]. The lift vector can then, for example, be expressed as

$$a_L = L\, R_{\bar{v}}(\mu)\, e_2. \tag{24}$$

where $R_{\bar{v}}(\mu)$ is the axis-angle rotation matrix of angle μ around the normalized velocity vector $\bar{v}$.

The dynamics (15) of the parallel transport frame expressed in terms of rotation matrices can also be expressed in terms of quaternions, for a more efficient numerical implementation. The extended dynamics of (r, v, R) could also be expressed in an $\mathrm{SE}_2(3)$ form [21] or as dual quaternions [22].

The advantages of the proposed approach are then illustrated in the following example of simulation of a vehicle performing a looping.

5 Illustration

This section is dedicated to a simple illustrative example of 3-DOF simulation of a toy lifting vehicle using a parallel transport frame to express the lift.

The vehicle considered here is moving in 3D on a flat Earth and is only subject to a constant gravity and a lift force that act as a control. No drag force is considered here, for simplicity and without loss of generality. A trajectory of the vehicle performing a looping is shown in Figure 2, and is detailed next.

The vehicle is starting at the origin of the reference frame (green point) with an initial velocity along the x-axis

$$r_0 = (0, 0, 0)^\top, \qquad v_0 = (V_0, 0, 0)^\top. \tag{25}$$

The parallel transport frame is initialized as $R_0 = I$ which satisfies (14). For readability, only the e_2 (orange) and e_3 (yellow) vectors of the parallel transport frame are shown .

The trajectory (blue) is obtained by numerical integration of (4) and (15) and is divided into the following phases. For each phase, a constant lift force is applied in a particular direction (purple) in the (e_2, e_3) plane.

1) First, the vehicle flies at constant altitude with the lift compensating the gravity.
2) Then, a lift force is applied in the direction of e_3 until vertical flight is achieved.
3) Vertical flight is then maintained for a small duration by not applying any lift.
4) A lift force is again applied in the direction of e_3 until the vehicle is again flying horizontally.
5) Afterwards, a lift force is applied in a direction combining e_2 and e_3, until the loop is achieved and the flight is again horizontal.
6) The last phase is at constant altitude, like the first one.

The following remarks can be made.

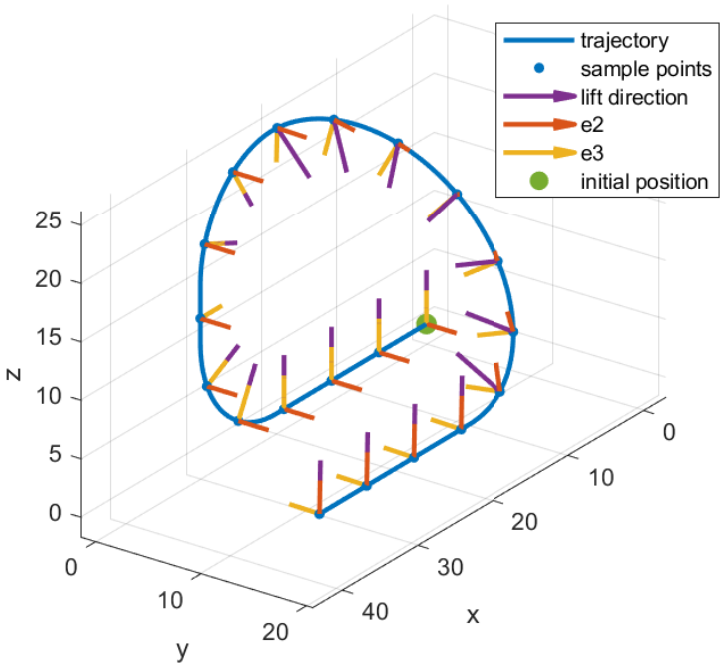

Fig. 2 Illustrative trajectory (blue) of a lifting vehicle performing a looping. The lift vector (direction in purple) is expressed in a parallel transport frame (orange and yellow) carried along the trajectory.

The plane (e_2, e_3) is always normal to the velocity vector and allows to describe the lift vector at any time along the trajectory. In particular, both vertical and horizontal flight is possible with this model, without a change of coordinate chart (in spherical coordinates) or reference direction (in Cartesian coordinates).

In the horizontal flight phases the frame does not rotate because the total acceleration of the vehicle is zero. The frame also does not rotate during the vertical flight phase because only the gravity applies and is colinear to the velocity.

As stated before, the frame is not periodic in general [16]. The initial and final parallel transport frames are indeed different. This is not of significant importance in practice because in order to recover an intuitive representation, one can always compute the bank angle (when well-defined) from the lift vector and the local vertical .

6 Conclusion

A model using parallel transport frame to express the lift vector without singularities in Cartesian coordinates has been presented and illustrated. This model intends to improve the generation and optimization of lifting vehicle trajectories by getting rid of singularity protection mechanisms that make them more complex.

Future works consist in demonstrating the interest of this model for trajectory optimization with direct shooting methods and successive convex optimization. A remaining challenge lies in removing the singularity at zero velocity, which has not been addressed in this paper.

Declaration of Use of Artificial Intelligence

Artificial intelligence was not used in the work presented.

References

[1] Erwin Mooij. Motion of a vehicle in a planetary atmosphere. *NASA STI/Recon Technical Report N*, 96:11743, 1994.

[2] Riccardo Bonalli, Bruno Hérissé, and Emmanuel Trélat. Optimal control of endoatmospheric launch vehicle systems: Geometric and computational issues. *IEEE Transactions on Automatic Control*, 65(6):2418–2433, 2019.

[3] Prince Edorh, Bruno Hérissé, and Eric Bourgeois. Glide back recovery of a winged reusable launch vehicle with wind estimate. In *EUCASS-3AF 2022*, 2022.

[4] Juan Carlos Hernández Ramírez and Meyer Nahon. A gravity-referenced moving frame for vehicle path following applications in 3d. *IEEE Robotics and Automation Letters*, 6(3):4393–4400, 2021.

[5] Qianjun Zhang, Yongzhuo Gao, Siyuan Meng, Hui Dong, Changhai Ru, and Wei Dong. A novel contouring control method based on optimal vector-referenced moving frame for 3d trajectory with zero curvature. *IEEE Transactions on Automation Science and Engineering*, 2024.

[6] John T Betts. *Practical methods for optimal control and estimation using nonlinear programming*. SIAM, 2010.

[7] Jean Frédéric Frenet. Sur les courbes à double courbure. *Journal de mathématiques pures et appliquées*, 17:437–447, 1852.

[8] Joseph Alfred Serret. Sur quelques formules relatives à la théorie des courbes à double courbure. *Journal de mathématiques pures et appliquées*, 16:193–207, 1851.

[9] Wolfgang Kühnel. *Differential geometry*, volume 77. American Mathematical Soc., 2015.

[10] Richard L Bishop. There is more than one way to frame a curve. *The American Mathematical Monthly*, 82(3):246–251, 1975.

[11] Fopke Klok. Two moving coordinate frames for sweeping along a 3d trajectory. *Computer Aided Geometric Design*, 3(3):217–229, 1986.

[12] Wenping Wang, Bert Jüttler, Dayue Zheng, and Yang Liu. Computation of rotation minimizing frames. *ACM Transactions on Graphics (TOG)*, 27(1):1–18, 2008.

[13] Heinrich Guggenheimer. Computing frames along a trajectory. *Computer Aided Geometric Design*, 6(1):77–78, 1989.

[14] Rida T Farouki. *Pythagorean—hodograph curves*. Springer, 2008.

[15] Rida T Farouki, Carlotta Giannelli, Maria Lucia Sampoli, and Alessandra Sestini. Rotation-minimizing osculating frames. *Computer Aided Geometric Design*, 31(1):27–42, 2014.

[16] Natasha Bosanac and Giuliana Miceli. Curve-based axes for specifying maneuvers in a multi-body system.

[17] Wenping Wang and Barry Joe. Robust computation of the rotation minimizing frame for sweep surface modeling. *Computer-Aided Design*, 29(5):379–391, 1997.

[18] Isaac Kaminer, António Pascoal, Enric Xargay, Naira Hovakimyan, Chengyu Cao, and Vladimir Dobrokhodov. Path following for small unmanned aerial vehicles using L1 adaptive augmentation of commercial autopilots. *Journal of guidance, control, and dynamics*, 33(2):550–564, 2010.

[19] Thomas Raffler, Jian Wang, and Florian Holzapfel. Path generation and control for unmanned multirotor vehicles using nonlinear dynamic inversion and pseudo control hedging. *IFAC Proceedings Volumes*, 46(19):194–199, 2013.

[20] Yi Zhu, Xin Chen, and Chuntao Li. A moving frame trajectory tracking method of a flying-wing UAV using the differential geometry. *International Journal of Aerospace Engineering*, 2016(1):3406256, 2016.

[21] Axel Barrau and Silvere Bonnabel. The invariant extended Kalman filter as a stable observer. *IEEE Transactions on Automatic Control*, 62(4):1797–1812, 2016.

[22] Unsik Lee and Mehran Mesbahi. Dual quaternions, rigid body mechanics, and powered-descent guidance. In *2012 51st IEEE Conference on Decision and Control (CDC)*, pages 3386–3391. IEEE, 2012.